



HAL
open science

Nonstandard anti-windup approach for event-triggered control purpose

Carla de Souza, Sophie Tarbouriech, Isabelle Queinnec, Antoine Girard

► **To cite this version:**

Carla de Souza, Sophie Tarbouriech, Isabelle Queinnec, Antoine Girard. Nonstandard anti-windup approach for event-triggered control purpose. *Systems and Control Letters*, 2024, 185, pp.105715. 10.1016/j.sysconle.2024.105715 . hal-04378600

HAL Id: hal-04378600

<https://hal.science/hal-04378600>

Submitted on 8 Jan 2024

HAL is a multi-disciplinary open access archive for the deposit and dissemination of scientific research documents, whether they are published or not. The documents may come from teaching and research institutions in France or abroad, or from public or private research centers.

L'archive ouverte pluridisciplinaire **HAL**, est destinée au dépôt et à la diffusion de documents scientifiques de niveau recherche, publiés ou non, émanant des établissements d'enseignement et de recherche français ou étrangers, des laboratoires publics ou privés.

Nonstandard anti-windup approach for event-triggered control purpose

Carla de Souza^a, Sophie Tarbouriech^{b,*}, Isabelle Queinnec^b and Antoine Girard^c

^a*Leyfa Measurement une filiale SNCF, Toulouse, France*

^b*LAAS-CNRS, Université de Toulouse, CNRS, Toulouse, France*

^c*Université Paris-Saclay, CNRS, CentraleSupélec, Laboratoire des Signaux et Systèmes, 91190, Gif-sur-Yvette, France, Paris, France*

ARTICLE INFO

Keywords:

Event-triggered control
Anti-windup
Linear matrix inequalities
Dynamic event-triggering mechanism

ABSTRACT

This paper aims at designing both a nonstandard anti-windup action and an event-triggering mechanism that reduce the transmission activity on the network while preserving the asymptotic stability of a linear system under a dynamic output-feedback controller. The event-triggering policy is based on the use of an additional internal dynamic variable. The nonstandard anti-windup term, which uses the difference between the transmitted and the current control output, is added to the controller structure to further save the communication resources. Sufficient conditions in terms of matrix inequalities are proposed to compute the anti-windup gain and the triggering parameters while avoiding the Zeno behavior. Numerical algorithms with feasibility guarantees allow to reduce the amount of data transmissions. Through numerical examples, we illustrate the efficacy of the proposed approach.

1. Introduction


In the traditional digital control framework, the control signal is transmitted periodically, independently from the output of the system. Such a time-triggering paradigm may result in redundant transmissions, as many of them are not really necessary to achieve stability and some performance properties. As an alternative, the event-triggered control (ETC) technique updates the system input only when a certain condition is verified. In this sense, the ETC copes with communication, energy consumption and computational constraints [9, 18]. Two general categories classify the existing approaches, namely, emulation-based and co-design approaches. In the former, the controller is a priori known and only the event-triggering policies have to be designed [24]. On the other hand, the last one simultaneously designs the control law and the event-triggering rules [2]. In this work, we consider the emulation approach. However, to further save the communication resources, we also propose to modify the initial control law by designing an additional nonstandard anti-windup action, added to the controller structure.

Over the years, several kinds of event-triggering policies have been proposed in the literature. Among them, the most commonly used consists of a static rule (see, for example, [10, 26, 12, 5]). By adding an internal dynamic variable into the previous one, we have an augmented rule with dynamics (see, for example, [7, 22]). Previous results show that the guaranteed lower bound on inter-executions times using a dynamic rule cannot be smaller than that obtained for a static rule [7], which motivates us to consider such a structure. A challenging issue that arises in this context is the avoidance of the Zeno-behavior (i.e. the high frequency of sampling). [11, 12] directly ensure a lower-bound for the inter-event times of the system under the event-triggering strategy. [14, 1, 22] propose a practical solution, which consists of using an explicit tuning parameter playing the role of a minimal dwell-time.

Based on the above, the main contributions of the current paper rely on: *i*) the design of a nonstandard anti-windup action to further reduce the number of data transmissions on the communication network, *ii*) the design of a dynamic event-triggering mechanism that uses only local information and avoids the Zeno-behavior by admitting an explicitly tuning parameter *iii*) the development of algorithms that allow computing both the anti-windup gain (directly or indirectly) and the triggering parameters while reducing the control signal updates. The proposed approach applies to

* This work has been supported by ANR under the project HANDY number 18-CE40-0010.

*Corresponding author

 carla.souza93@hotmail.com (C. de Souza); tarbour@laas.fr (S. Tarbouriech); isabelle.queinnec@laas.fr (I. Queinnec); antoine.girard@12s.centralesupelec.fr (A. Girard)

ORCID(s): 0000-0002-9790-7877 (C. de Souza); 0000-0002-0816-5614 (S. Tarbouriech); 0000-0003-0783-1977 (I. Queinnec); 0000-0002-4075-9041 (A. Girard)

continuous-time systems stabilized by dynamic output-feedback controllers. In this case, the nonstandard anti-windup term, consisting of a gain multiplied by the difference between the transmitted and current controller output, is used as a new input to the controller structure. This scheme is different from the classical event-based scheme since in the classical case the difference between the transmitted and current controller output does not affect the dynamic of the controller. By using the Lyapunov theory, we formulate sufficient conditions, in terms of matrix inequalities, with feasibility guarantees and prevention of the Zeno effects. Those are incorporated into the optimization algorithms, which effectively deal with minimizing the triggering activity. It is then illustrated how this simple augmentation, if suitably tuned, can dramatically reduce the number of control updates on the closed-loop system response. The classical case can be simply recovered by removing the anti-windup-like loop.

The paper is organized as follows. Section 2 describes the closed-loop topology considered, showing the nonstandard anti-windup term and the dynamic event-triggering policy. Such a section also presents the problem we intend to solve. In Section 3, we first show a result (Theorem 1) proposed by [22], which is vital to prove the asymptotic stability of the closed-loop system with the dynamic triggering mechanism. After that, we present the main result of the paper (Theorem 2), which computes both the anti-windup gain and the triggering parameters while preserving the closed-loop stability. A particular result (Corollary 3) is also given at the end of this section. In Section 4, optimization algorithms are established to minimize the transmission activity on the communication network. The first one incorporates the main condition and sets some constraints for the variables. On the other hand, the second one, uses the concave-convex methodology [6] to find the anti-windup gain without imposing any structure to the slacks variables, which happens in Theorem 2. Section 5 illustrates the efficacy of the proposal using two numerical examples. Finally, in Section 6, some concluding remarks and potential future works are pointed out.

Notation. \mathbb{N} , \mathbb{R}^n , $\mathbb{R}^{n \times m}$ denote respectively the sets of nonnegative integers, n -dimensional vectors and $n \times m$ matrices. For any matrix A , A^\top denotes its transpose. For any square matrix A , $\text{trace}(A)$ denotes its trace and $\text{He}\{A\} = A + A^\top$. $\text{diag}(A_1; A_2)$ is a diagonal matrix with block diagonal matrices A_1 and A_2 . For two symmetric matrices of the same dimensions, A and B , $A > B$ means that $A - B$ is symmetric positive definite. For a vector $x \in \mathbb{R}^q$, the notation $x \geq 0$ means that x is a nonnegative vector, that is, all its components are nonnegative: $x_{(i)} \geq 0$, $i = 1, \dots, q$, and $x \in \mathbb{R}_{\geq 0}^q$. $\mathbf{1}$ and $\mathbf{0}$ stand respectively for the identity and the null matrix of appropriate dimensions. For a partitioned matrix, the symbol \star stands for symmetric blocks. $\|\cdot\|$ stands for the Euclidean norm. $|\cdot|$ stands for the absolute value. For any vector $x \in \mathbb{R}^n$ and any symmetric positive definite (or semi-positive definite) matrix, $\|x\|_Q^2$ denotes the quadratic form $x^\top Q x$.

2. Problem Statement

2.1. System description

Consider the following continuous-time linear plant

$$\begin{cases} \dot{x}_p(t) &= A_p x_p(t) + B_p u(t), \\ y_p(t) &= C_p x_p(t), \end{cases} \quad (1)$$

where $x_p(t) \in \mathbb{R}^{n_p}$, $u(t) \in \mathbb{R}^m$, $y_p(t) \in \mathbb{R}^p$ are the state, the input and the output of the plant, respectively. Matrices A_p , B_p , C_p are constant, known and of appropriate dimensions. Pairs (A_p, B_p) and (C_p, A_p) are supposed to be controllable and observable, respectively.

We consider an output feedback controller to stabilize the plant (1) and therefore to drive the output to zero. This controller is defined by:

$$\begin{cases} \dot{x}_c(t) &= A_c x_c(t) + B_c y_p(t), \\ y_c(t) &= C_c x_c(t) + D_c y_p(t), \end{cases} \quad (2)$$

where $x_c(t) \in \mathbb{R}^{n_c}$ and $y_c(t) \in \mathbb{R}^m$ are the state and the output of the controller. Thus, the closed loop resulting from the connection of system (1) with the controller (2) through $u(t) = y_c(t)$ is supposed to be asymptotically stable. In

other words, the matrix of the linear closed loop $A = \begin{bmatrix} A_p + B_p D_c C_p & B_p C_c \\ B_c C_p & A_c \end{bmatrix}$ is supposed to be Hurwitz.

However, the plant and the controller are supposed to be implemented through a network and then are considered to be in separate nodes. At instants determined by an event generator, a sample of the controller output (y_c) is sent to the

plant, and then the input signal for the plant is

$$u(t_k) = y_c(t_k). \quad (3)$$

Then, the control input u is implemented through a sample-and-hold mechanism, meaning that it is not continuously updated or transmitted to the actuators. Indeed, it is updated at certain instants $\{t_k\}_{k \in \mathbb{N}}$, which form a sequence of strictly increasing positive scalars. Control action is held constant between two successive sampling instants (t_k and t_{k+1}) through a zero order holder. Differently from classical digital control approaches, the sampling interval $t_{k+1} - t_k$ is not assumed to be constant but can be seen as an additional control action.

Then, the closed loop reads:

$$\begin{cases} \dot{x}_p(t) = A_p x_p(t) + B_p y_c(t_k), \\ y_p(t) = C_p x_p(t), \\ \dot{x}_c(t) = A_c x_c(t) + B_c y_p(t) + \theta_1(t), \\ y_c(t) = C_c x_c(t) + D_c y_p(t), \end{cases} \quad (4)$$

for all $t \in [t_k, t_{k+1})$. It involves an additional input $\theta_1(t)$ to be designed by taking inspiration from anti-windup action (see, for example [21] in the context of saturation nonlinearity) for mitigating the undesired effect of the sampling of $y_c(t)$. The implicit objective is to add some degree of freedom in order to reduce the number of updates of the control induced by the event-triggering mechanism, while preserving the stability and some performance of the closed loop.

By using a similar formulation as in [18] we define the available vector for event-triggering purpose $\delta(t)$:

$$\delta(t) = y_c(t_k) - y_c(t). \quad (5)$$

Thus, $\delta(t)$ depends only on the output of the controller and is then available at the controller node. Indeed, the function $\delta(t)$ represents a measure of the difference between the computed continuous-time controller output value and its sampled and held version sent to implement the control. Therefore, the idea behind the use of a nonstandard anti-windup action is to use this difference δ as a new input of the controller and then to consider the following signal $\theta_1(t)$ to augment the controller:

$$\theta_1(t) = E_c(y_c(t_k) - y_c(t)) = E_c \delta(t), \quad (6)$$

with $E_c \in \mathbb{R}^{n_c \times m}$ a matrix to be designed. A representation of the scheme considered is illustrated in Figure 1.

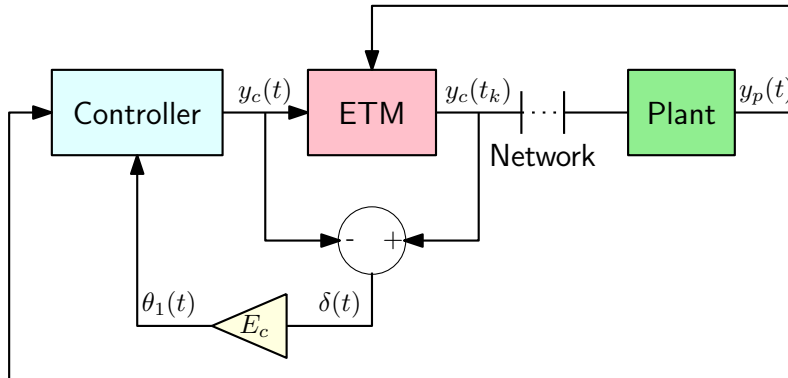


Figure 1: Block diagram of the closed-loop system.

By defining the augmented state vector $x = [x_p^\top \quad x_c^\top]^\top \in \mathbb{R}^n$, $n = n_p + n_c$, the closed loop can be expressed as follows:

$$\begin{cases} \dot{x}(t) = Ax(t) + (B + RE_c)\delta(t), \\ y(t) = Cx(t), \\ y_c(t) = Kx(t), \end{cases} \quad (7)$$

with

$$\begin{aligned} A &= \begin{bmatrix} A_p + B_p D_c C_p & B_p C_c \\ B_c C_p & A_c \end{bmatrix}, \quad B = \begin{bmatrix} B_p \\ \mathbf{0} \end{bmatrix}, \quad C = \begin{bmatrix} C_p & \mathbf{0} \\ D_c C_p & C_c \end{bmatrix}, \\ K &= \begin{bmatrix} D_c C_p & C_c \end{bmatrix}, \quad \text{and } R = \begin{bmatrix} \mathbf{0} \\ 1 \end{bmatrix}. \end{aligned} \quad (8)$$

for all $t \in [t_k, t_{k+1})$. By construction the closed-loop matrix A defined in (8) is Hurwitz. The scheme proposed in (7) is different from the classical event-based scheme (where u is updated) since in the classical case δ does not appear in the dynamic of the controller. Hence the idea here is to use the knowledge we have about this signal δ in order to mitigate the effect of the event-triggered control. The classical case is recovered by setting $E_c = 0$.

2.2. Event-triggering mechanism

By taking inspiration from [22], the event-triggered implementation of the controller (2) is proposed through a dynamic event triggering mechanism (ETM) to enrich the event generator algorithm managing the controller to decide when the control input has to be updated, based on the available information. That can be viewed as an expansion of the event-triggered control strategy proposed in [22], [23] and [7]. Then, we consider that a dynamic event-triggering mechanism is introduced through an internal dynamic variable denoted $\eta \in \mathbb{R}$, following the impulsive dynamics:

$$\begin{cases} \dot{\eta}(t) &= f(y(t), \delta(t), \eta(t)), \\ &\forall t \in [t_k, t_k + T) \cup (t_k + T, t_{k+1}), \\ \eta(t_k + T) &= \max(0, \eta(t_k + T^-)), \end{cases} \quad (9)$$

for all $k \in \mathbb{N}$, where $f : \mathbb{R}^{p+2m+1} \rightarrow \mathbb{R}$ and $\eta(t_k + T^-)$ denotes the limit of $\eta(t)$ when t approaches $t_k + T$ from below. It is further assumed that the dynamic variable η is initialized to a value $\eta(t_0) \geq 0$. Leveraging this dynamics (9), the sampling instants are determined from the following logic:

$$t_{k+1} = \min\{t \geq t_k + T, \text{ s.t. } \eta(t) \leq 0\}, \quad (10)$$

where T is a positive scalar. By definition, (10) guarantees that the next sampling time will occur at least T time units ahead the last one. As T can be seen as a minimal dwell time, the avoidance of Zeno solutions is guaranteed and the dwell time T ensures that no sampling can occur in the interval $[t_k, t_k + T)$. Furthermore, for $t \geq t_k + T$ the control is not updated before $\eta(t) \leq 0$.

The main problem we intend to solve can be summarized as follows:

Problem 1. Given a positive scalar T , design the anti-windup gain E_c and devise function f , such that the event-triggering mechanism defined as in (10) and (9), ensures the asymptotic stability of the closed-loop system (7), while reducing the number of events generated.

Remark 1. More sophisticated functions for the triggering logic used in equation (10) could be used, by replacing the condition $\eta(t) \leq 0$ by a more sophisticated $g(y, \delta, \eta) \leq 0$, with, for instance, $g(y, \delta, \eta) = \eta + \sigma(\|y\|_{Q_{f1}}^2 - \|\delta\|_{Q_{f2}}^2)$. However, this kind of functions g may not result in larger inter-execution times as discussed in [7]. Furthermore, another additional objective could be to handle a performance index as in [17] or [7].

3. Sufficient stability conditions for ETM design

3.1. Auxiliary result

Solving Problem 1 resides in designing E_c and f in order to ensure the asymptotic stability of the sampled-data system (7). To do this, we use Theorem 1 of [22], which is also inspired from [19], [20] and can be viewed as a general formulation of [13]. This theorem is recalled below.

Theorem 1. [22] *Given a positive scalar T , if there exist a function $V : \mathbb{R}^n \rightarrow \mathbb{R}$, scalars $\epsilon_1 > 0$, $\epsilon_2 > 0$, $\epsilon_3 > 0$ and $1 > \epsilon_4 > 0$ such that:*

$$1. \quad \epsilon_1 \|x\|^2 \leq V(x(t)) \leq \epsilon_2 \|x\|^2, \forall x \in \mathbb{R}^n$$

2. $\eta(t_k) \geq 0$ and $\eta(t) \geq 0$,
 $\forall t \in [t_k + T, t_{k+1}), \forall k \in \mathbb{N}$
3. $\dot{V}(x(t)) + \dot{\eta}(t) \leq -\epsilon_3(V(x(t)) + \eta(t))$,
 $\forall t \in [t_k, t_k + T) \cup (t_k + T, t_{k+1}), \forall k \in \mathbb{N}$
4. $V(x(t_k + T)) - V(x(t_k)) \leq -\epsilon_4 V(x(t_k)), \forall k \in \mathbb{N}$

then, the closed-loop system (7) with the triggering mechanism (10) and (9) is asymptotically stable and the inter-sampling times are lower bounded by T .

3.2. Theoretical conditions

In this section, leveraging on Theorem 1, we present numerical techniques to explicitly design E_c and function f such that the assumptions of Theorem 1 hold. With this aim, we focus on function f described below:

$$f(y, \delta, \eta) = \|y\|_{Q_{f1}}^2 - \|\delta\|_{Q_{f2}}^2 - Q_{f3}\eta \quad (11)$$

with $\mathbf{0} < Q_{f1} = Q_{f1}^\top \in \mathbb{R}^{(m+p) \times (m+p)}$, $\mathbf{0} < Q_{f2} = Q_{f2}^\top \in \mathbb{R}^{m \times m}$ and $0 < Q_{f3} \in \mathbb{R}$. In order to address Problem 1, we need to design Q_{f1} , Q_{f2} , Q_{f3} , E_c and the function V complying with the items of Theorem 1. Indeed, we expand Theorem 2 in [22] to co-design the anti-windup gain E_c and the event-triggering mechanism.

Let us first define the following useful matrices

$$\begin{aligned} M_{1d} &= \begin{bmatrix} \mathbf{1} & \mathbf{0} & \mathbf{0} \end{bmatrix}, M_{2d} = \begin{bmatrix} \mathbf{0} & \mathbf{1} & \mathbf{0} \end{bmatrix}, M_{3d} = \begin{bmatrix} \mathbf{0} & \mathbf{0} & \mathbf{1} \end{bmatrix}, M_{4d} = \begin{bmatrix} \mathbf{1} & \mathbf{0} & -\mathbf{1} \end{bmatrix}, \\ M_{5d} &= \begin{bmatrix} A - BK & -\mathbf{1} & BK \end{bmatrix}, M_{6d} = \begin{bmatrix} A - (B + RE_c)K & -\mathbf{1} & (B + RE_c)K \end{bmatrix}, \end{aligned} \quad (12)$$

in order to propose the following general result.

Theorem 2. Given a positive scalar T . If there exist symmetric positive definite matrices $P \in \mathbb{R}^{n \times n}$, $Q_{f1} \in \mathbb{R}^{(m+p) \times (m+p)}$, $Q_{f2} \in \mathbb{R}^{m \times m}$, $Q_{f3} \in \mathbb{R}^{1 \times 1}$, $\Omega \in \mathbb{R}^{n \times n}$, symmetric matrices $F_1 \in \mathbb{R}^{n \times n}$ and $G \in \mathbb{R}^{n \times n}$, matrices $Z \in \mathbb{R}^{n_c \times m}$, $Y_1 \in \mathbb{R}^{n \times n}$, $Y_2 \in \mathbb{R}^{n \times n}$, $F_2 \in \mathbb{R}^{n \times n}$ and $N \in \mathbb{R}^{3n \times n}$, and scalars $\epsilon_3 > 0$ and $\rho > 0$, such that the following relations hold

$$\begin{bmatrix} Y_1^\top A + A^\top Y_1 + C^\top Q_{f1} C + \epsilon_3 P & A^\top Y_2 - Y_1^\top + P & Y_1^\top B + RZ & \mathbf{0} \\ \star & -Y_2 - Y_2^\top & Y_2^\top B + \rho RZ & \mathbf{0} \\ \star & \star & -Q_{f2} & \mathbf{0} \\ \star & \star & \star & -Q_{f3} + \epsilon_3 \end{bmatrix} \leq \mathbf{0}, \quad (13)$$

$$\begin{aligned} \Psi_0 &= He\{M_{1d}^\top P M_{2d}\} - M_{4d}^\top F_1 M_{4d} - He\{M_{4d}^\top F_2 M_{3d}\} + He\{-N M_{4d}\} + T(M_{2d}^\top \Omega M_{2d} \\ &+ He\{M_{2d}^\top F_1 M_{4d}\} + He\{M_{2d}^\top F_2 M_{3d}\} + M_{3d}^\top G M_{3d}) + He\left\{ \begin{bmatrix} Y_1^\top \\ Y_2^\top \\ \mathbf{0} \end{bmatrix} M_{5d} - \begin{bmatrix} \mathbf{1} \\ \rho \mathbf{1} \\ \mathbf{0} \end{bmatrix} RZ K M_{4d} \right\} < \mathbf{0}, \end{aligned} \quad (14)$$

$$\Psi_T = \begin{bmatrix} He\{M_{1d}^\top P M_{2d}\} - T M_{3d}^\top G M_{3d} - M_{4d}^\top F_1 M_{4d} \\ -He\{M_{4d}^\top F_2 M_{3d}\} + He\{-N M_{4d}\} \\ + He\left\{ \begin{bmatrix} Y_1^\top \\ Y_2^\top \\ \mathbf{0} \end{bmatrix} M_{5d} - \begin{bmatrix} \mathbf{1} \\ \rho \mathbf{1} \\ \mathbf{0} \end{bmatrix} RZ K M_{4d} \right\} & TN \\ TN^\top & -T\Omega \end{bmatrix} < \mathbf{0}, \quad (15)$$

with Y_1 and Y_2 structured as follows, respectively:

$$Y_1 = \begin{bmatrix} Y_{111} & Y_{112} \\ \mathbf{0} & Y_{22} \end{bmatrix} \text{ and } Y_2 = \begin{bmatrix} Y_{211} & Y_{212} \\ \mathbf{0} & \rho Y_{22} \end{bmatrix}. \quad (16)$$

Then,

- i) The items of Theorem 1 hold with $V(x) = x^\top Px$, and function f is defined as in (11) from Q_{f1} , Q_{f2} , Q_{f3} ;
- ii) The inter-sampling times are lower bounded by T ;
- iii) The anti-windup gain solution to Problem 1 is given by $E_c = (Y_{22}^\top)^{-1} Z$.

Proof. Consider the function $V(x) = x^\top Px$, with $P = P^\top > 0$. Item 1) of Theorem 1 is satisfied with $\epsilon_1 = \lambda_{\min}(P)$ and $\epsilon_2 = \lambda_{\max}(P)$.

By (9), we have $\eta(t_k + T) \geq 0$. From continuity of η on $[t_k + T, t_{k+1}]$, (10) gives that $\eta(t) \geq 0$ for all $t \in [t_k + T, t_{k+1}]$. Together with $\eta(t_0) \geq 0$, this guarantees the satisfaction of item 2) of Theorem 1.

By computing the time-derivative of $\mathcal{W}(x, \eta) = V(x) + \eta$, for any $t \in [t_k, t_k + T) \cup (t_k + T, t_{k+1})$, along the closed-loop system (7) with the dynamics of η defined by (9) and (11) one gets: $\dot{\mathcal{W}}(x, \eta) = \dot{V}(x) + \dot{\eta} = \dot{x}^\top Px + x^\top P\dot{x} + \dot{\eta}$. Or equivalently by defining

$$\xi = \begin{bmatrix} x^\top & \dot{x}^\top & \delta^\top & \sqrt{|\eta|} \end{bmatrix}^\top,$$

one gets:

$$\dot{\mathcal{W}}(x, \eta) = \xi^\top \left(He \left\{ \begin{bmatrix} \mathbf{1} \\ \mathbf{0} \\ \mathbf{0} \\ \mathbf{0} \end{bmatrix} P \begin{bmatrix} \mathbf{0} & \mathbf{1} & \mathbf{0} & \mathbf{0} \end{bmatrix} \right\} + \mathbb{C}^\top Q_f \mathbb{C} \right) \xi, \quad (17)$$

with $\mathbb{C} = \begin{bmatrix} C & \mathbf{0} & \mathbf{0} & \mathbf{0} \\ \mathbf{0} & \mathbf{0} & \mathbf{1} & \mathbf{0} \\ \mathbf{0} & \mathbf{0} & \mathbf{0} & \mathbf{1} \end{bmatrix}$ and $Q_f = \begin{bmatrix} Q_{f1} & \mathbf{0} & \mathbf{0} \\ \mathbf{0} & -Q_{f2} & \mathbf{0} \\ \mathbf{0} & \mathbf{0} & -Q_{f3} \end{bmatrix}$. Furthermore, note that from (7) one verifies:

$$\begin{bmatrix} A & -\mathbf{1} & B + RE_c & \mathbf{0} \end{bmatrix} \xi = M_0 \xi = 0.$$

Then one can satisfy the following condition for matrices Y_1 and Y_2 :

$$He \left\{ \xi^\top \begin{bmatrix} Y_1^\top \\ Y_2^\top \\ \mathbf{0} \\ \mathbf{0} \end{bmatrix} M_0 \xi \right\} = 0. \quad (18)$$

Hence, satisfying $\dot{\mathcal{W}}(x, \eta) < 0$ along the trajectories of system (7), is equivalent to satisfy:

$$\begin{aligned} \mathcal{L}_1 &= \dot{\mathcal{W}}(x, \eta) + He \left\{ \xi^\top \begin{bmatrix} Y_1^\top \\ Y_2^\top \\ \mathbf{0} \\ \mathbf{0} \end{bmatrix} M_0 \xi \right\} \\ &= \xi^\top \left(He \left\{ \begin{bmatrix} Y_1^\top \\ Y_2^\top \\ \mathbf{0} \\ \mathbf{0} \end{bmatrix} M_0 + M_1^\top P M_2 \right\} + \mathbb{C}^\top Q_f \mathbb{C} \right) \xi < 0 \end{aligned}$$

with $M_1 = \begin{bmatrix} \mathbf{1} & \mathbf{0} & \mathbf{0} & \mathbf{0} \end{bmatrix}$ and $M_2 = \begin{bmatrix} \mathbf{0} & \mathbf{1} & \mathbf{0} & \mathbf{0} \end{bmatrix}$.

In order to linearize the terms in which E_c is involved, that is $Y_1^\top RE_c$ and $Y_2^\top RE_c$ hidden in (18), we impose the following structure to the multipliers:

$$Y_1 = \begin{bmatrix} Y_{111} & Y_{112} \\ \mathbf{0} & Y_{22} \end{bmatrix} \text{ and } Y_2 = \begin{bmatrix} Y_{211} & Y_{212} \\ \mathbf{0} & \rho Y_{22} \end{bmatrix}, \quad (19)$$

which leads to

$$Y_1^\top RE_c = \begin{bmatrix} \mathbf{0} \\ Y_{22}^\top E_c \end{bmatrix} = RZ, \quad Y_2^\top RE_c = \begin{bmatrix} \mathbf{0} \\ \rho Y_{22}^\top E_c \end{bmatrix} = \rho RZ,$$

with the change of variable $Z = Y_{22}^\top E_c$. Hence, \mathcal{L}_1 reads:

$$\mathcal{L}_1 = \xi^\top \begin{bmatrix} Y_1^\top A + A^\top Y_1 + C^\top Q_{f1} C & A^\top Y_2 - Y_1^\top + P & Y_1^\top B + RZ & \mathbf{0} \\ \star & -Y_2 - Y_2^\top & Y_2^\top B + \rho RZ & \mathbf{0} \\ \star & \star & -Q_{f2} & \mathbf{0} \\ \star & \star & \star & -Q_{f3} \end{bmatrix} \xi = \xi^\top \Phi \xi.$$

Hence, if relation (13) is satisfied, then it follows that

$$\mathcal{L}_1 = \xi^\top \Phi \xi + \epsilon_3 x^\top P x + \epsilon_3 |\eta| \leq 0$$

thus,

$$\dot{W} \leq -\epsilon_3 x^\top P x - \epsilon_3 |\eta| \leq -\epsilon_3 (x^\top P x + \eta)$$

and item 3) in Theorem 1 is satisfied. Note that the satisfaction of relation (13) implies that matrix Y is non-singular and therefore due to the structure of Y as considered in (16), Y_{22} is also non-singular.

In order to prove that item 4) of Theorem 1 holds, one has to consider (7) over the interval $[t_k, t_k + T]$. To do this, we consider the system trajectories of (7) in a lifted domain [15, 25, 4], expanding the approach in [13]. Thus, by defining $\tau = t - t_k$, with $\tau \in [0, T]$, and a function $X_k(\tau) = x(t_k + \tau) = x(t)$, from (7) one gets the following equation:

$$\dot{X}_k(\tau) = (A - (B + RE_c)K)X_k(\tau) + (B + RE_c)KX_k(0). \quad (20)$$

Furthermore, for $t \in [t_k, t_k + T]$, one can write:

$$V(x(t)) = V(X_k(\tau)) = X_k(\tau)^\top P X_k(\tau), \quad \tau \in [0, T]. \quad (21)$$

The solution to (20) for $\tau \in [0, T]$ lives in $\mathbb{F}_{[0, T]}^{2n}$, which is the set of differentiable functions from the interval $[0, T]$ into \mathbb{R}^{2n} . Then for this solution $X_k \in \mathbb{F}_{[0, T]}^{2n}$ one can define:

$$W(\tau, X_k) = V(X_k(\tau)) + V_0(\tau, X_k), \quad (22)$$

with $V_0(\tau, X_k) : [0, T] \rightarrow \mathbb{F}_{[0, T]}^{2n}$ being a looped-functional borrowed from [16], [15]. Hence, let us consider

$$\begin{aligned} V_0(\tau, X_k) &= (T - \tau)(X_k(\tau) - X_k(0))^\top F_1(X_k(\tau) - X_k(0)) \\ &\quad + (T - \tau)((X_k(\tau) - X_k(0))^\top F_2 X_k(0) + X_k(0)^\top F_2^\top (X_k(\tau) - X_k(0))) \\ &\quad + (T - \tau)\tau X_k(0)^\top G X_k(0) + (T - \tau) \int_0^\tau \dot{X}_k(\theta)^\top \Omega \dot{X}_k(\theta) d\theta. \end{aligned} \quad (23)$$

It follows that V_0 verifies a looping condition: $V_0(T, X_k) = V_0(0, X_k) = 0, \forall X_k \in \mathbb{F}_{[0, T]}^{2n}$. Then the time-derivative of $W(\tau, X_k)$ (i.e. $\frac{dW}{d\tau}$ here) along the trajectories of (20) reads:

$$\begin{aligned} \dot{W}(\tau, X_k) &= 2X_k(\tau)^\top P \dot{X}_k(\tau) + (T - \tau)\dot{X}_k(\tau)^\top [\Omega \dot{X}_k(\tau) + 2F_1(X_k(\tau) - X_k(0)) + 2F_2 X_k(0)] \\ &\quad - (X_k(\tau) - X_k(0))^\top [F_1(X_k(\tau) - X_k(0)) + 2F_2 X_k(0)] + (T - 2\tau)X_k(0)^\top G X_k(0) \\ &\quad - \int_0^\tau \dot{X}_k(\theta)^\top \Omega \dot{X}_k(\theta) d\theta. \end{aligned} \quad (24)$$

By defining the augmented vector $\xi_k(\tau) = [X_k(\tau)^\top \quad \dot{X}_k(\tau)^\top \quad X_k(0)^\top]^\top$, one can consider the following constraint similarly to the first part of the proof:

$$He \left\{ \xi_k(\tau)^\top \begin{bmatrix} Y_1^\top \\ Y_2^\top \\ \mathbf{0} \end{bmatrix} M_{6d} \xi_k(\tau) \right\} = 0. \quad (25)$$

with M_{6d} defined in (12). Hence, in order to linearize the terms in which E_c is involved, that is $Y_1^\top R E_c K$ and $Y_2^\top R E_c K$, we impose the same structure to the multipliers as in (19). That leads by using the same change of variables as in the continuous part of the proof:

$$Y_1^\top R E_c K = \begin{bmatrix} \mathbf{0} \\ Y_{22}^\top E_c K \end{bmatrix} = R Z K, \quad Y_2^\top R E_c K = \begin{bmatrix} \mathbf{0} \\ \rho Y_{22}^\top E_c K \end{bmatrix} = \rho R Z K, \quad (26)$$

with $Z = Y_{22}^\top E_c$. Furthermore, from [15, 3], the integral term can be upper-bounded as follows

$$- \int_0^\tau \dot{X}_k(\theta)^\top \Omega \dot{X}_k(\theta) d\theta \leq -2\xi_k(\tau)^\top N (X_k(\tau) - X_k(0)) + \tau \xi_k(\tau)^\top N \Omega^{-1} N^\top \xi_k(\tau),$$

for any matrix $N \in \mathbb{R}^{3n \times n}$. Then, the time-derivative of function W satisfy:

$$\begin{aligned} \dot{W}(\tau, X_k) \leq & \xi_k(\tau) \left(He\{M_{1d}^\top P M_{2d}\} + (T - \tau)(M_{2d}^\top \Omega M_{2d} + He\{M_{2d}^\top F_1 M_{4d}\} \right. \\ & + He\{M_{2d}^\top F_2 M_{3d}\}) + He\left\{ \begin{bmatrix} Y_1^\top \\ Y_2^\top \\ \mathbf{0} \end{bmatrix} M_{6d} \right\} - M_{4d}^\top F_1 M_{4d} - He\{M_{4d}^\top F_2 M_{3d}\} \\ & \left. + (T - 2\tau)M_{3d}^\top G M_{3d} + He\{-N M_{4d}\} + \tau N \Omega^{-1} N^\top \right) \xi_k(\tau). \end{aligned} \quad (27)$$

with M_{1d} , M_{2d} , M_{3d} , M_{4d} and M_{6d} defined in (12). We can observe that the expression in the right-hand side of (27) is affine with respect to τ . Since $\tau \in [0, T]$, by convexity arguments, it suffices to ensure that the right-hand-side of (27) is negative for $\tau = 0$ and for $\tau = T$ to guarantee that $\dot{W}(\tau, X_k) < 0$, $\forall \tau \in [0, T]$. Nothing that, similarly to the continuous case, one has

$$He\left\{ \begin{bmatrix} Y_1^\top \\ Y_2^\top \\ \mathbf{0} \end{bmatrix} M_{6d} \right\} = He\left\{ \begin{bmatrix} Y_1^\top \\ Y_2^\top \\ \mathbf{0} \end{bmatrix} M_{5d} - \begin{bmatrix} \mathbf{1} \\ \rho \mathbf{1} \\ \mathbf{0} \end{bmatrix} R Z K M_{4d} \right\}$$

with M_{5d} defined in (12), thus the negativity of $\dot{W}(\tau, X_k)$ is ensured whenever the following inequalities are satisfied:

$$\begin{aligned} \Psi_0 = & He\{M_{1d}^\top P M_{2d}\} - M_{4d}^\top F_1 M_{4d} - He\{M_{4d}^\top F_2 M_{3d}\} + He\{-N M_{4d}\} + T(M_{2d}^\top \Omega M_{2d} \\ & + He\{M_{2d}^\top F_1 M_{4d}\} + He\{M_{2d}^\top F_2 M_{3d}\} + M_{3d}^\top G M_{3d}) + He\left\{ \begin{bmatrix} Y_1^\top \\ Y_2^\top \\ \mathbf{0} \end{bmatrix} M_{5d} - \begin{bmatrix} \mathbf{1} \\ \rho \mathbf{1} \\ \mathbf{0} \end{bmatrix} R Z K M_{4d} \right\} < \mathbf{0}, \end{aligned}$$

$$\Psi_T = \begin{bmatrix} He\{M_{1d}^\top P M_{2d}\} - T M_{3d}^\top G M_{3d} - M_{4d}^\top F_1 M_{4d} \\ -He\{M_{4d}^\top F_2 M_{3d}\} + He\{-N M_{4d}\} \\ + He\left\{ \begin{bmatrix} Y_1^\top \\ Y_2^\top \\ \mathbf{0} \end{bmatrix} M_{5d} - \begin{bmatrix} \mathbf{1} \\ \rho \mathbf{1} \\ \mathbf{0} \end{bmatrix} R Z K M_{4d} \right\} \\ T N \\ T N^\top \\ -T \Omega \end{bmatrix} < \mathbf{0},$$

which correspond to relations (14) and (15). Thus, the satisfaction of relations (14) and (15) ensures that $\dot{W}(\tau, X_k) < 0$. In other words, one gets

$$\int_0^T \dot{W}(\tau, X_k) d\tau = V(X_k(T)) - V(X_k(0)) + V_0(T, X_k) - V_0(0, X_k) = V(X_k(T)) - V(X_k(0)) < 0$$

since by definition $V_0(T, X_k) = V_0(0, X_k)$. We can conclude that the satisfaction of relations (14) and (15) ensures that

$$V(X_k(T)) - V(X_k(0)) = V(x(t_k + T)) - V(x(t_k)) < 0, \forall k \in \mathbb{N}.$$

Hence, there exists $0 < \epsilon_4 < 1$ such that item 4) of Theorem 1 holds. \square

Theorem 1 uses particular structures of the multipliers Y_1 and Y_2 (see equation (19) in order to have an easy way to compute the event-triggering parameters Q_{f1} , Q_{f2} , Q_{f3} and the anti-windup-like gain E_c . The remaining parameters ϵ_3 and ρ are tuning parameters: ϵ_3 can be fixed sufficiently small and ρ can be searched via a grid search. Nevertheless, if the anti-windup gain E_c is fixed a priori, we have no need to structure the multipliers as suggested in the corollary below and therefore no need of a tuning parameter ρ .

Corollary 3. *Given a positive scalar T and an anti-windup gain E_c . If there exist symmetric positive definite matrices $P \in \mathbb{R}^{n \times n}$, $Q_{f1} \in \mathbb{R}^{(m+p) \times (m+p)}$, $Q_{f2} \in \mathbb{R}^{m \times m}$, $Q_{f3} \in \mathbb{R}^{1 \times 1}$, and $\Omega \in \mathbb{R}^{n \times n}$, symmetric matrices $F_1 \in \mathbb{R}^{n \times n}$, $G \in \mathbb{R}^{n \times n}$, matrices $Z \in \mathbb{R}^{n_c \times m}$, $Y_1 \in \mathbb{R}^{n \times n}$, $Y_2 \in \mathbb{R}^{n \times n}$, $Y_3 \in \mathbb{R}^{n \times m}$, $Y_4 \in \mathbb{R}^{n \times 1}$, $Y_5 \in \mathbb{R}^{n \times n}$, $F_2 \in \mathbb{R}^{n \times n}$ and $N \in \mathbb{R}^{3n \times n}$, and a scalar $\epsilon_3 > 0$, such that the following relations hold*

$$\begin{bmatrix} He\{Y_1^\top A\} + C^\top Q_{f1} C + \epsilon_3 P & A^\top Y_2 - Y_1^\top + P & A^\top Y_3 + Y_1^\top (B + RE_c) & A^\top Y_4 \\ \star & He\{-Y_2\} & -Y_3 + Y_2^\top (B + RE_c) & -Y_4 \\ \star & \star & He\{Y_3^\top (B + RE_c)\} - Q_{f2} & Y_4^\top (B + RE_c) \\ \star & \star & \star & -Q_{f3} + \epsilon_3 \end{bmatrix} < \mathbf{0}, \quad (28)$$

$$\begin{aligned} \Psi_0 = & He\{M_{1d}^\top P M_{2d}\} - M_{4d}^\top F_1 M_{4d} - He\{M_{4d}^\top F_2 M_{3d}\} + He\{-N M_{4d}\} + He\left\{\begin{bmatrix} Y_1^\top \\ Y_2^\top \\ Y_5^\top \end{bmatrix} M_{6d}\right\} \\ & + T(M_{2d}^\top \Omega M_{2d} + He\{M_{2d}^\top F_1 M_{4d}\} + He\{M_{2d}^\top F_2 M_{3d}\} + M_{3d}^\top G M_{3d}) < \mathbf{0}, \end{aligned} \quad (29)$$

$$\Psi_T = \begin{bmatrix} He\{M_{1d}^\top P M_{2d}\} - M_{4d}^\top F_1 M_{4d} - He\{M_{4d}^\top F_2 M_{3d}\} \\ + He\{-N M_{4d}\} + He\left\{\begin{bmatrix} Y_1^\top \\ Y_2^\top \\ Y_5^\top \end{bmatrix} M_{6d}\right\} - T M_{3d}^\top G M_{3d} & TN \\ TN^\top & -T\Omega \end{bmatrix} < \mathbf{0}. \quad (30)$$

with M_{id} , $i = 1, \dots, 6$, defined in (12). Then,

- i) The items of Theorem 1 hold with $V(x) = x^\top P x$, and the function f is defined as in (11) from Q_{f1} , Q_{f2} , Q_{f3} .
- ii) The inter-sampling times are lower bounded by T .

Proof. The proof of Corollary 3 follows the same steps as Theorem 2, except for the fact that we consider more slack variables Y_1 , Y_2 , Y_3 , Y_4 , and Y_5 without any particular structure. \square

Remark 2. Since in Corollary 3, the anti-windup gain E_c is fixed, one can consider any value, in particular, the case without anti-windup action, i.e. $E_c = \mathbf{0}$.

Remark 3. When E_c is given, as an alternative to Corollary 3, the conditions in [22, Thm2] could be adopted by considering (7) over the interval $[t_k, t_k + T]$, handling a discrete-time system with an exponential matrix involving E_c .

4. Optimization procedures

4.1. Minimization of the transmission data rate

There does not exist a simple and direct optimal way to reduce the amount of control updates, but some indirect and heuristic algorithms can be used. Let us recall that the control is updated when $\eta(t)$ becomes negative. Hence, an

indirect way to reduce the control updates is to delay the time at which η will start to be negative. By following a greedy heuristic an intuitive way to do this consists then in maximizing $\dot{\eta}$. From (11), such a maximization will be based on playing with matrices Q_{f1} , Q_{f2} , Q_{f3} , or more precisely to maximize $\text{trace}(Q_{f1})$ and to minimize $\text{trace}(Q_{f2}, Q_{f3})$. It is important to observe that the equation (11) is homogeneous then one can normalize the matrices Q_{f1} , Q_{f2} , Q_{f3} . Furthermore, Q_{f3} is directly related to the convergence rate of η : smaller is Q_{f3} slower is the convergence of the dynamics but there are few event-triggering instants; Moreover since Q_{f3} is bounded by ϵ_3 from relation (13), a way to proceed is to fix Q_{f3} close to ϵ_3 , that is small enough. Then one has to optimize $\text{trace}(Q_{f1})$ or $\text{trace}(Q_{f2})$. In the paper we chose to minimize $\text{trace}(Q_{f2})$. In this sense, the following optimization problems can then be considered:

$$\mathcal{O}_1 : \begin{cases} \min & \theta, \\ \text{subject to} & (i), (j), (k), \text{trace}(Q_{f2}) \leq \theta \mathbf{1}, \theta > 0, \\ & \text{trace}(Q_{f1}) \geq \mu \mathbf{1} \text{ and } \text{trace}(Q_{f2}) \geq \text{trace}(Q_{f3}), \end{cases} \quad (31)$$

with μ a given normalization parameter, $(i) = (13)$, $(j) = (14)$ and $(k) = (15)$ for Theorem 2, and $(i) = (28)$, $(j) = (29)$ and $(k) = (30)$ for Corollary 3. Note that, if Corollary 3 is used to improve the results of Theorem 2, we can then use the matrix Q_{f1} obtained from Theorem 2 as a lower bound to the one searched in Corollary 3.

4.2. Convex-concave algorithm

As commented before Corollary 3, conditions proposed in Theorem 2 suffer from some conservatism due to the particular structure imposed on the slack variables Y_1 and Y_2 to avoid bi-linearity between design variables. To overcome this drawback, we can use the concave-convex decomposition approach proposed by [6]. Thus, such an approach proposes to express bi-linear terms via concave-convex decomposition, which is always possible. In this way, as long as an initial feasible point is available, the concave terms are linearized around this feasible point. From this, the resulting linearized problem is solved, and the solution obtained is then used to linearize the original concave terms again. This basically leads to a sequence of semidefinite programming (SDP) problems that can be solved iteratively.

To apply this approach, as a first step, we rewrite (13), (14) and (15) in the following equivalent linear-bilinear decomposed forms:

$$\underbrace{\begin{bmatrix} Y_1^\top A + A^\top Y_1 + C^\top Q_{f1} C + \epsilon_3 P & A^\top Y_2 - Y_1^\top + P & Y_1^\top B & \mathbf{0} \\ \star & -Y_2 - Y_2^\top & Y_2^\top B & \mathbf{0} \\ \star & \star & -Q_{f2} & \mathbf{0} \\ \star & \star & \star & -Q_{f3} + \epsilon_3 \end{bmatrix}}_{\mathcal{L}_1(P, Y_1, Y_2, Q_f)} + He \left\{ \underbrace{\begin{bmatrix} Y_1^\top \\ Y_2^\top \\ \mathbf{0} \\ \mathbf{0} \end{bmatrix}}_{\mathcal{X}_1^\top(Y_1, Y_2)} \underbrace{\begin{bmatrix} \mathbf{0} & \mathbf{0} & RE_c & \mathbf{0} \end{bmatrix}}_{\mathcal{Y}_1(E_c)} \right\} < \mathbf{0}, \quad (32)$$

$$\begin{aligned}
 \Psi_0 = & \underbrace{He\{M_{1d}^\top P M_{2d}\} - M_{4d}^\top F_1 M_{4d} - He\{M_{4d}^\top F_2 M_{3d}\} + He\{-N M_{4d}\} + T(M_{2d}^\top \Omega M_{2d})}_{\mathcal{L}_2(P, Y_1, Y_2)} \\
 & + He\{M_{2d}^\top F_1 M_{4d}\} + He\{M_{2d}^\top F_2 M_{3d}\} + M_{3d}^\top G M_{3d} + He\left\{\begin{bmatrix} Y_1^\top \\ Y_2^\top \\ \mathbf{0} \end{bmatrix} M_{5d}\right\} \\
 & + He\left\{\begin{bmatrix} Y_1^\top \\ Y_2^\top \\ \mathbf{0} \end{bmatrix} \underbrace{\begin{bmatrix} -RE_c K & \mathbf{0} & RE_c K \end{bmatrix}}_{\mathcal{Y}_2(E_c)}\right\}_{\mathcal{X}_2^\top(Y_1, Y_2)} < \mathbf{0}, \tag{33}
 \end{aligned}$$

$$\begin{aligned}
 \Psi_T = & \underbrace{\begin{bmatrix} He\{M_{1d}^\top P M_{2d}\} - T M_{3d}^\top G M_{3d} + He\left\{\begin{bmatrix} Y_1^\top \\ Y_2^\top \\ \mathbf{0} \end{bmatrix} M_{5d}\right\} & T N \\ -M_{4d}^\top F_1 M_{4d} - He\{M_{4d}^\top F_2 M_{3d}\} + He\{-N M_{4d}\} & -T \Omega \\ & T N^\top \end{bmatrix}}_{\mathcal{L}_3(P, Y_1, Y_2)} \\
 & + He\left\{\begin{bmatrix} Y_1^\top \\ Y_2^\top \\ \mathbf{0} \\ \mathbf{0} \end{bmatrix} \underbrace{\begin{bmatrix} -RE_c K & \mathbf{0} & RE_c K & \mathbf{0} \end{bmatrix}}_{\mathcal{Y}_3(E_c)}\right\}_{\mathcal{X}_3^\top(Y_1, Y_2)} < \mathbf{0}. \tag{34}
 \end{aligned}$$

The last term in the previous inequalities can be equivalently rewritten in a convex-concave decomposed form, by dropping the dependency on the decision variables, as follows:

$$\mathcal{L}_i + \mathcal{X}_i^\top \mathcal{X}_i + \mathcal{Y}_i^\top \mathcal{Y}_i - (\mathcal{X}_i - \mathcal{Y}_i)^\top (\mathcal{X}_i - \mathcal{Y}_i) < \mathbf{0}, \quad i = 1, 2, 3. \tag{35}$$

By applying Schur complement, (35) is equivalent to:

$$\begin{bmatrix} \mathcal{L}_i - \mathcal{X}_i^\top \mathcal{X}_i - \mathcal{Y}_i^\top \mathcal{Y}_i + He\{\mathcal{X}_i^\top \mathcal{Y}_i\} & \mathcal{X}_i^\top & \mathcal{Y}_i^\top \\ \star & -\mathbf{1} & \mathbf{0} \\ \star & \star & -\mathbf{1} \end{bmatrix} < \mathbf{0}, \quad i = 1, 2, 3. \tag{36}$$

The last step consists of computing the differential of the concave terms:

$$\begin{aligned}
 \mathcal{Q}_1 &= -\mathcal{X}_1^\top \mathcal{X}_1 - \mathcal{Y}_1^\top \mathcal{Y}_1 + He\{\mathcal{X}_1^\top \mathcal{Y}_1\} = \\
 &\quad \begin{bmatrix} -Y_1^\top Y_1 & -Y_1^\top Y_2 & Y_1^\top RE_c & \mathbf{0} \\ \star & -Y_2^\top Y_2 & Y_2^\top RE_c & \mathbf{0} \\ \star & \star & -E_c^\top R^\top RE_c & \mathbf{0} \\ \star & \star & \star & \mathbf{0} \end{bmatrix}, \\
 \mathcal{Q}_2 &= -\mathcal{X}_2^\top \mathcal{X}_2 - \mathcal{Y}_2^\top \mathcal{Y}_2 + He\{\mathcal{X}_2^\top \mathcal{Y}_2\} = \\
 &\quad \begin{bmatrix} -Y_1^\top Y_1 - He\{Y_1^\top RE_c K\} & -Y_1^\top Y_2 & Y_1^\top RE_c K \\ -K^\top E_c^\top R^\top RE_c K & -K^\top E_c^\top R^\top Y_2 & +K^\top E_c^\top R^\top RE_c K \\ \star & -Y_2^\top Y_2 & Y_2^\top RE_c \\ \star & \star & K^\top E_c^\top R^\top RE_c K \end{bmatrix}, \\
 \mathcal{Q}_3 &= -\mathcal{X}_3^\top \mathcal{X}_3 - \mathcal{Y}_3^\top \mathcal{Y}_3 + He\{\mathcal{X}_3^\top \mathcal{Y}_3\} = \\
 &\quad \begin{bmatrix} \mathcal{Q}_2 & \mathbf{0} \\ \star & \mathbf{0} \end{bmatrix},
 \end{aligned} \tag{37}$$

which, by using the notation $h = (h_{Y_1}, h_{Y_2}, h_{E_c})$ with $h_{Y_1} = (Y_1 - Y_{10})$, $h_{Y_2} = (Y_2 - Y_{20})$ and $h_{E_c} = (E_c - E_{c0})$, are given by:

$$\begin{aligned}
 D\mathcal{Q}_1(Y_{10}, Y_{20}, E_{c0})h &= \\
 &\quad \begin{bmatrix} -He\{Y_1^\top h_{Y_1}\} & -h_{Y_1}^\top Y_2 & h_{Y_1}^\top RE_c & \mathbf{0} \\ \star & \mathbf{0} & \mathbf{0} & \mathbf{0} \\ \star & \star & \mathbf{0} & \mathbf{0} \\ \star & \star & \star & \mathbf{0} \end{bmatrix} + \begin{bmatrix} \mathbf{0} & -Y_1^\top h_{Y_2} & \mathbf{0} & \mathbf{0} \\ \star & -He\{Y_2^\top h_{Y_2}\} & h_{Y_2}^\top RE_c & \mathbf{0} \\ \star & \star & \mathbf{0} & \mathbf{0} \\ \star & \star & \star & \mathbf{0} \end{bmatrix} + \\
 &\quad \begin{bmatrix} \mathbf{0} & \mathbf{0} & Y_1^\top Rh_{E_c} & \mathbf{0} \\ \star & \mathbf{0} & Y_2^\top Rh_{E_c} & \mathbf{0} \\ \star & \star & -He\{E_c^\top R^\top Rh_{E_c}\} & \mathbf{0} \\ \star & \star & \star & \mathbf{0} \end{bmatrix}, \\
 D\mathcal{Q}_2(Y_{10}, Y_{20}, E_{c0})h &= \\
 &\quad \begin{bmatrix} -He\{Y_1^\top h_{Y_1}\} - He\{h_{Y_1}^\top RE_c K\} & -h_{Y_1}^\top Y_2 & h_{Y_1}^\top RE_c K \\ \star & \mathbf{0} & \mathbf{0} \\ \star & \star & \mathbf{0} \end{bmatrix} + \begin{bmatrix} \mathbf{0} & -Y_1^\top h_{Y_2} & \mathbf{0} \\ \star & -He\{Y_2^\top h_{Y_2}\} & h_{Y_2}^\top RE_c K \\ \star & \star & \mathbf{0} \end{bmatrix} + \\
 &\quad \begin{bmatrix} -He\{Y_1^\top Rh_{E_c} K\} & -K^\top h_{E_c}^\top R^\top Y_2 & Y_1^\top Rh_{E_c} K \\ -He\{K^\top E_c^\top R^\top Rh_{E_c} K\} & He\{K^\top E_c^\top R^\top Rh_{E_c} K\} \\ \star & \mathbf{0} & Y_2^\top Rh_{E_c} K \\ \star & \star & He\{K^\top E_c^\top R^\top Rh_{E_c} K\} \end{bmatrix}, \\
 D\mathcal{Q}_3(Y_{10}, Y_{20}, E_{c0})h &= \begin{bmatrix} D\mathcal{Q}_2(Y_{10}, Y_{20}, E_{c0})h & \mathbf{0} \\ \mathbf{0} & \mathbf{0} \end{bmatrix},
 \end{aligned}$$

At this point, given (Y_{10}, Y_{20}, E_{c0}) , the ‘‘linear inner approximation’’ of the optimization problem (31) around (Y_{10}, Y_{20}, E_{c0}) reads:

$$\mathcal{O}_2 : \begin{cases} \min & \theta, \\ \text{subject to} & \mathcal{M}_i(P, Y_1, Y_2, E_c | P, Y_{10}, Y_{20}, E_{c0}) < \mathbf{0}, \text{ with } i = 1, 2, 3, \\ & \text{trace}(\mathcal{Q}_{f_2}) \leq \theta \mathbf{1}, \theta > 0, \text{ trace}(\mathcal{Q}_{f_1}) \geq \mu \mathbf{1}, \text{ and} \\ & \text{trace}(\mathcal{Q}_{f_2}) \geq \text{trace}(\mathcal{Q}_{f_3}). \end{cases} \tag{38}$$

where:

$$\underbrace{\begin{bmatrix} \mathcal{R}_i(P, Y_1, Y_2, E_c | P, Y_{10}, Y_{20}, E_{c0}) & \mathcal{W}_i(Y_1, Y_2, E_c) \\ \star & -\mathbf{1} \end{bmatrix}}_{\mathcal{M}_i(P, Y_1, Y_2, E_c | P, Y_{10}, Y_{20}, E_{c0})} < \mathbf{0}, \quad i = 1, 2, 3,$$

and

$$\begin{aligned} \mathcal{R}_i(P, Y_1, Y_2, E_c | P, Y_{10}, Y_{20}, E_{c0}) &:= \mathcal{L}_i(P, Y_1, Y_2, E_c) + \mathcal{Q}(Y_{10}, Y_{20}, E_{c0}) + \\ &\quad (D\mathcal{Q}(Y_{10}, Y_{20}, Y_{30}))h, \\ \mathcal{W}_i(Y_1, Y_2, E_c) &:= [\mathcal{X}_i^\top(Y_1, Y_2) \quad \mathcal{Y}_i^\top(E_c)] \end{aligned}$$

As discussed before (32), the applicability of the convex-concave decomposition enjoys interesting properties provided that an initial feasible solution exists. Let us then state the following result regarding the feasibility of the conditions of Corollary 3.

Proposition 4. *Conditions of Corollary 3 have feasible solution. Indeed, by selecting the following variables:*

$$\begin{aligned} Y_1 = P; Y_2 = \epsilon \mathbf{1}; Y_3 = 0; Y_4 = 0; Y_5 = 0; \epsilon_3 \leq \frac{\max(\operatorname{Re}(\lambda_i(A)))}{2}; Q_{f1} = \epsilon \mathbf{1}; E_c = 0; Q_{f2} > \frac{\epsilon}{2} B^\top B \\ Q_{f3} > \epsilon_3; F_1 = -C^\top Q_{f1} C - \epsilon_3 P; N = \begin{bmatrix} N_1 \\ N_2 \\ N_3 \end{bmatrix} = \begin{bmatrix} -PBK \\ -\epsilon BK \\ -\frac{K^\top Q_{f2} K}{4} + F_1 \end{bmatrix}; F_2 = F_2^T = F_1 - N_3 \end{aligned} \quad (39)$$

one can ensure the existence of sufficiently small positive scalars T, ϵ , matrices G, Ω such that relations (28), (29), (30) hold.

Proof. Let us start with the feasibility of relation (28) with the proposed selection in (39). The matrix in the left-hand term of (28), denoted here as M_c reads:

$$M_c = \begin{bmatrix} A^\top P + PA + C^\top Q_{f1} C + \epsilon_3 P & \epsilon A^\top & PB & \mathbf{0} \\ \star & -2\epsilon \mathbf{1} & \epsilon B & \mathbf{0} \\ \star & \star & -Q_{f2} & \mathbf{0} \\ \star & \star & \star & -Q_{f3} + \epsilon_3 \end{bmatrix}, \quad (40)$$

To study the feasibility we focus on the upper-left sub-matrix which consists in the three first rows and columns (denoted \bar{M}_c) since $-Q_{f3} + \epsilon_3 < \mathbf{0}$. Recall that matrix A is Hurwitz by construction. The feasibility of \bar{M}_c is indeed related to the feasibility of the upper-left sub-matrix which consists in the two first rows and columns. Hence by applying the Schur complement and invoking the fact that A is Hurwitz, this sub-matrix is feasible since it is always possible to choose ϵ small enough such that $A^\top P + PA + C^\top Q_{f1} C + \epsilon_3 P + \frac{\epsilon}{2} A^\top A < \mathbf{0}$. Let us now consider the feasibility of relations (29) and (30), therefore the matrices Ψ_0 and Ψ_T . With the selection (39), one gets for Ψ_0 :

$$\Psi_0 = \begin{bmatrix} A^\top P + PA + C^\top Q_{f1} C + \epsilon_3 P & \epsilon A^\top & \mathbf{0} \\ \star & -2\epsilon \mathbf{1} & \mathbf{0} \\ \star & \star & -(K^\top Q_{f2} K + C^\top Q_{f1} C + \epsilon_3 P) \end{bmatrix} + T M_0 \quad (41)$$

with M_0 corresponding to all the terms in parenthesis in (29). And by using the Schur complement one can write Ψ_T as:

$$\Psi_T = \begin{bmatrix} A^\top P + PA + C^\top Q_{f1} C + \epsilon_3 P & \epsilon A^\top & \mathbf{0} \\ \star & -2\epsilon \mathbf{1} & \mathbf{0} \\ \star & \star & -(K^\top Q_{f2} K + C^\top Q_{f1} C + \epsilon_3 P) \end{bmatrix} + T M_1 \quad (42)$$

with M_1 corresponding to the terms multiplied by T . Hence, it is clear that the feasibility of relation (28) with the considered selection (39) implies that the common matrix to Ψ_0 and Ψ_T is negative definite. Therefore there always exists a small enough positive scalar T making $\Psi_0 < \mathbf{0}$ and $\Psi_T < \mathbf{0}$. \square

From Proposition 4 the existence of an initial feasible solution is ensured for the original problem. Then, the convex-concave algorithm iterates from this initial feasible solution and never stops for infeasibility.

5. Numerical Examples

In this section, we use two examples to testify the efficacy of the proposed approach.

Academic Example: This example is borrowed from [8]. Consider system (1) with the following matrices:

$$A_p = \begin{bmatrix} -1.5 & 1 \\ 1 & 0 \end{bmatrix} \quad B_p = \begin{bmatrix} 1 \\ 0 \end{bmatrix} \quad \text{and} \quad C_p = [0 \quad 1], \quad (43)$$

and a PI stabilizing controller described by

$$A_c = 0, \quad B_c = -1, \quad C_c = 0.15 \quad \text{and} \quad D_c = -3. \quad (44)$$

Note that the matrix A_p is unstable since its eigenvalues are 2 and -1 .

Our goal is to design an anti-windup gain and the triggering parameters that reduce the number of data transmissions on the network while maintaining the closed-loop stability. First, we solve the optimization procedure \mathcal{O}_1 in (31) with the conditions of Theorem 2. As they depend on the parameters T , ϵ_3 and ρ , we vary their values in certain intervals to examine their influence on the anti-windup gain E_c and the cost function θ . We find out that only ρ has a substantial impact on these variables, as can be seen in Figure 2.

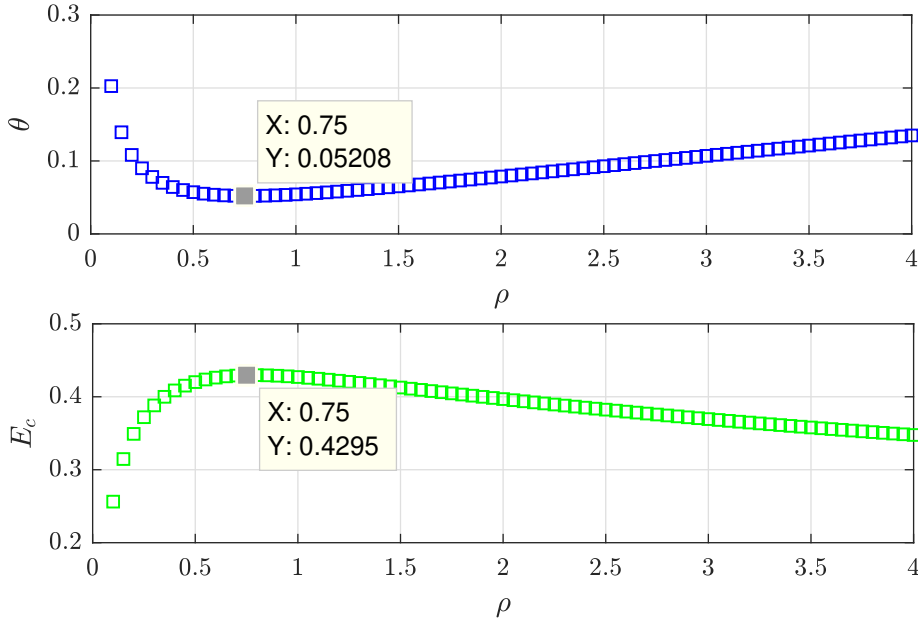


Figure 2: Influence of ρ on θ (on the top) and E_c (on the bottom).

Thus, we choose $\rho = 0.75$ to continue our studies, since it gives the smallest cost function. Observe that such a value also gives the highest anti-windup gain. The other parameters are set at $T = 0.02$ and $\epsilon_3 = 10^{-4}$. In this case, we find the following anti-windup gain and triggering parameters:

$$E_c = 0.4295, \quad Q_{f1} = \begin{bmatrix} 9.0320 & 2.9570 \\ 2.9570 & 0.9681 \end{bmatrix}, \quad Q_{f2} = 0.0521, \quad Q_{f3} = 0.0344.$$

Then, we simulate the closed-loop system response on a frame of 100 seconds for 64 initial conditions obtained by varying x_1 and x_2 from -7 to 7 with steps of 2, $x_c(0) = 0$ and $\eta(0) = 0$. The red squares in Figure 3 indicate the number of updates of the control output. Note that the control signals were transmitted through the network on average at only 487 (red line) instants. Conditions of Corollary 3 may then be used in the optimization procedure \mathcal{O}_1 , with the

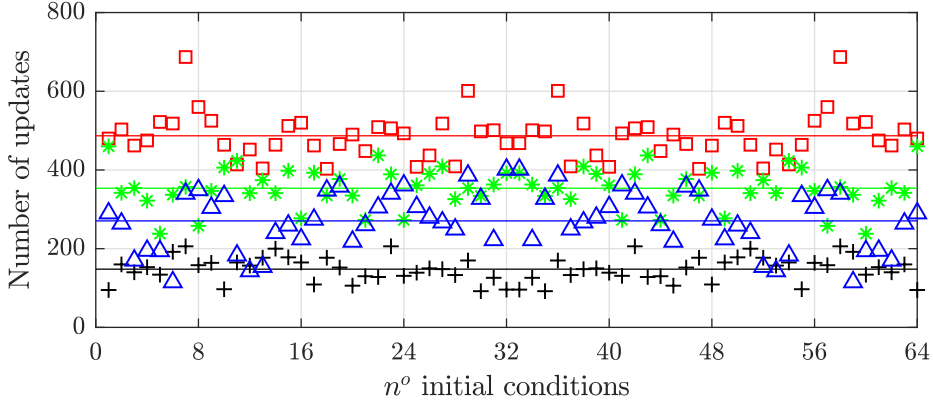


Figure 3: Evaluation of the number of updates for the cases: Theorem 2 (\square), Corollary 3 with $E_c \neq \mathbf{0}$ (+) and with $E_c = \mathbf{0}$ (*) and Concave-Convex technique (\triangle).

anti-windup gain previously obtained, allowing to obtain the triggering parameters:

$$Q_{f1} = \begin{bmatrix} 9.0411 & 2.9444 \\ 2.9444 & 0.9588 \end{bmatrix}, Q_{f2} = 0.0117, Q_{f3} = 0.0078.$$

Re-running the simulations, we got the number of updates indicated in Figure 3 by the black plus signals. The black line shows the average of these values, about 148, which represents a reduction of the transmission activity of almost 3 times compared to Theorem 2. Such a reduction illustrates the conservatism introduced in Theorem 2 to linearize the matrix inequalities, contrary to what is done in Corollary 3, in the case where E_c is given.

Furthermore, still employing Corollary 3, we test it with $E_c = \mathbf{0}$ to see the advantages of considering the nonstandard anti-windup gain. The results of this case are represented in Figure 3 by the green asterisks. We have an average of updates of about 354 (green line), which is higher than the one obtained with $E_c \neq \mathbf{0}$, thus confirming our intuition. In this case, we found the following triggering matrices:

$$Q_{f1} = \begin{bmatrix} 9.5617 & 2.0472 \\ 2.0472 & 0.4383 \end{bmatrix}, Q_{f2} = 0.4394, Q_{f3} = 0.2945.$$

Last, we design the anti-windup gain and the triggering parameters by using the concave-convex methodology. As this approach requires feasible initial matrices Y_1, Y_2 and P , we solved Corollary 3 with $E_c = \mathbf{0}, Y_3 = \mathbf{0}, Y_4 = \mathbf{0}$ and $Y_5 = \mathbf{0}$ to find them. From this, we obtained the matrices E_c and Q_f given below. By simulating the closed-loop system response for the same initial conditions, we get the number of updates represented in Figure 3 by the blue triangles. The average of these values is indicated by the blue line, about 271. Therefore, for this example, the concave convex algorithm was able to further reduce the transmission activity w.r.t. Theorem 2, but not as much as Corollary 3.

$$E_c = 0.0809, Q_{f1} = \begin{bmatrix} 9.4673 & 2.2459 \\ 2.2459 & 0.5328 \end{bmatrix}, Q_{f2} = 0.2962, Q_{f3} = 0.1974.$$

As a last evaluation, we plotted in Figure 4 the evolution in time of the functions $V(x)$ (blue line) and $\mathcal{W}(x, \eta)$ (red line) for the system initialized in $x_p(0) = [1 \ 1]^T$ and using the triggering policy obtained with Theorem 2. The values of $V(x)$ in the instants of transmission (blue squares) are highlighted with blue squares. One can check that the function $V(x)$ is not strictly decreasing, but it is upper-bounded by the function $\mathcal{W}(x, \eta)$, which is a decreasing function. Furthermore, we can observe that the dynamic event-triggering mechanism achieved a good compromise maximizing the inter-event times while minimizing the variations of $V(x)$.

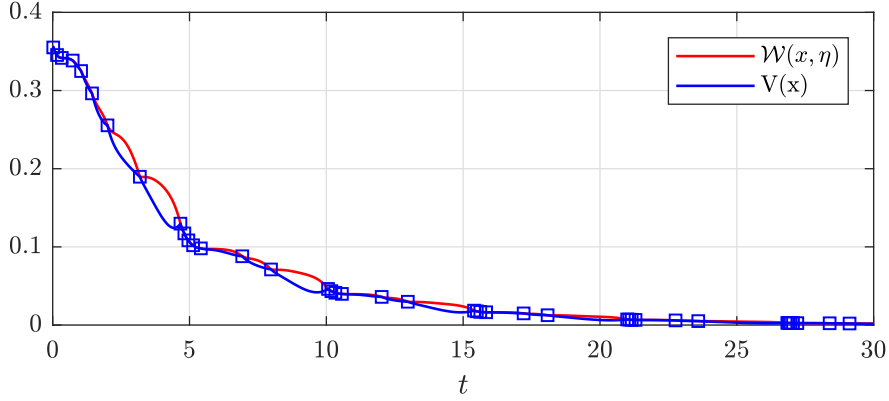


Figure 4: Evolution of the functions $W(x(t), \eta(t))$ (red line) and $V(x(t))$ (blue line).

F/A-18 HARV Aircraft Example: The dynamics of the F/A-18 HARV aircraft is described by the model (1) with the following matrices:

$$A_p = \begin{bmatrix} -2.3142 & 0.5305 & -15.5763 & 0 \\ -0.0160 & -0.1287 & 3.0081 & 0 \\ 0.0490 & -0.9980 & -0.1703 & 0.0440 \\ 1 & 0.0491 & 0 & 0 \end{bmatrix}, \quad B_p = \begin{bmatrix} 23.3987 & 21.4333 & 3.2993 \\ -0.1644 & 0.3313 & -1.9836 \\ -0.0069 & -0.0153 & 0.0380 \\ 0 & 0 & 0 \end{bmatrix},$$

$$C_p = \begin{bmatrix} 0 & 0 & 1 & 0 \\ 0 & 0 & 0 & 1 \end{bmatrix}.$$

This system can be stabilized through the dynamic output-feedback controller borrowed from [21], whose matrices are shown below:

$$A_c = \begin{bmatrix} -0.98 & 0.05 & -0.03 & -1.84 \\ 32.55 & -4.09 & 0.42 & -16.22 \\ 65.56 & -2.90 & -6.85 & -9.77 \\ 10.91 & 0.20 & -0.05 & -9.92 \end{bmatrix}, \quad B_c = \begin{bmatrix} 0.24 & -0.03 \\ 0.205 & -0.2897 \\ -46.23 & 0.89 \\ 1.59 & -0.14 \end{bmatrix},$$

$$C_c = \begin{bmatrix} 32.55 & -0.00 & -0.63 & -10.57 \\ 20.11 & 0.18 & -0.26 & -7.73 \\ -1.61 & -0.73 & -0.47 & 5.40 \end{bmatrix}, \quad D_c = \begin{bmatrix} -2.77 & -0.1 \\ -0.64 & -0.11 \\ -4.22 & 0.19 \end{bmatrix}.$$

Our objective is to design both an anti-windup gain and the triggering parameters that reduce the transmission activity on the network while preserving the closed-loop stability. To do this, we solve the optimization procedure \mathcal{O}_1 in (31) with the conditions of Theorem 2, $T = 0.08$, $\epsilon_3 = 1e^{-5}$, $\mu = 0.1$, and $\rho = 0.8$, finding the following anti-windup gain matrix

$$E_c = \begin{bmatrix} 0.0650 & 0.0206 & 0.0350 \\ 0.7775 & 0.5300 & 1.1094 \\ 3.1890 & 1.6636 & 11.3786 \\ 0.2239 & 0.1129 & 0.0282 \end{bmatrix}. \quad (45)$$

From this, we simulate the closed-loop system response on a frame of 6 seconds by considering the initial conditions $x_p(0) = [1500 \ 0 \ 0 \ 0]^T$, $x_c(0) = [0 \ 0 \ 0 \ 0]^T$ and $\eta(0) = 0$. In such a case, the number of control updates is 23, which corresponds to an update rate of approximately 31%, w.r.t what we would obtain with a constant sampling rate $T_c = 0.08$ s. Note that to fix identical values for T (dwell time) and T_c (sampling period in periodic case) corresponds

to interpret the ETM scheme as trying to increase the time before the next update with respect to what would do with a constant sampling. The percentage of update with respect to the constant sampling case of course depends on the duration of the simulation.

Then, to further reduce the transmission activity, we use the anti-windup gain (45) to solve the optimization procedure \mathcal{O}_1 with Corollary 3. With the new optimal \mathcal{Q}_f matrix, we re-simulated the closed-loop temporal response obtaining a number of control updates equal to 21 (28%).

Then, using the concave-convex method given by (38), where initial matrices Y_1 , Y_2 and P are solution of \mathcal{O}_1 with Corollary 3 and given initial matrices $E_c = \mathbf{0}$, $Y_3 = \mathbf{0}$, $Y_4 = \mathbf{0}$, and $Y_5 = \mathbf{0}$, we were able to design the anti-windup gain E_c and the triggering matrix \mathcal{Q}_f . By simulating the closed-loop system response, we got a number of control updates equal to 17 (23%), thus saving more network resources than the other technique, in this example.

To analyse the performance of the closed loop, we plot the plant outputs, the inter-events time, and the control signal of each case. Figure 5 shows the plant outputs $y_{p,1}(t)$ (on the top) and $y_{p,2}(t)$ (on the bottom) for the cases without ETM (green solid lines), Theorem 2 (red dashed lines), Corollary 3 (black dotted line) and Concave-Convex technique (blue dash-dotted line). Note that the system performance tends to deteriorate as the control signal update rate decreases. The

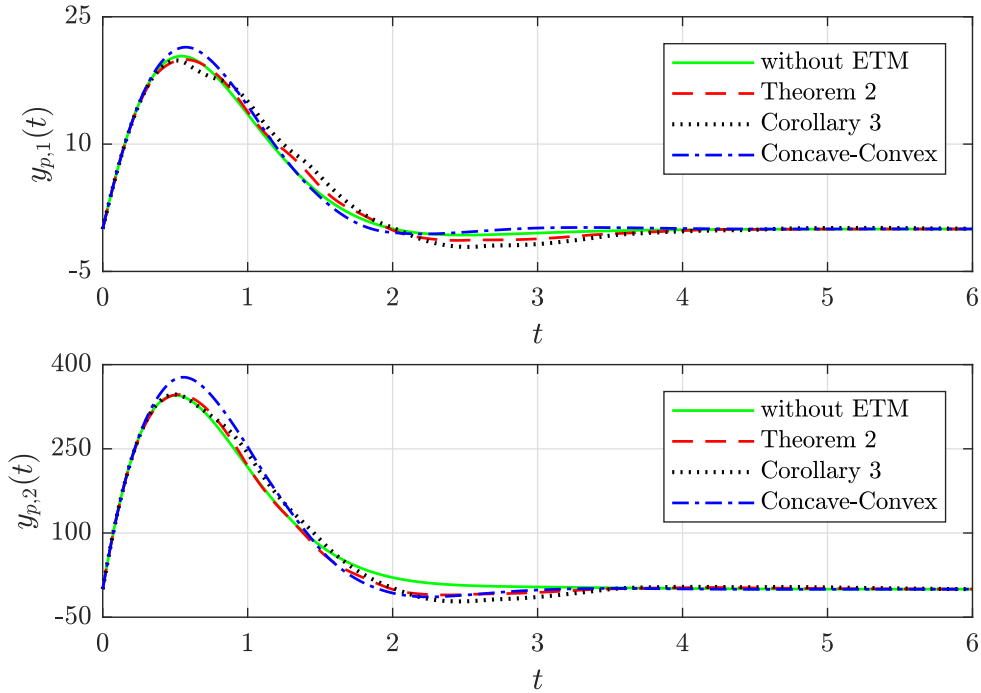


Figure 5: Plant output signals.

inter-event times of the ETMs for the cases without ETM, Theorem 2, Corollary 3 and Concave-Convex technique are shown in Figure 6, respectively. We can verify that the Concave-Convex technique actually achieves larger intervals without updating the control input than the other cases.

Figure 7 shows the control outputs $y_{c,1}(t_k)$ (on the top), $y_{c,2}(t_k)$ (on the middle), and $y_{c,3}(t_k)$ (on the bottom) for the cases without ETM, Theorem 2, Corollary 3 and Concave-Convex technique. We can see that in general more control effort is required when introducing ETMs into the closed loop.

6. Conclusions

This paper has proposed optimization algorithms for the design of a nonstandard anti-windup action and a dynamic event-triggering mechanism. They allow to reduce the number of control updates while maintaining the asymptotic stability of the closed loop system. Also, the Zeno effect is avoided whenever the sufficient conditions are attended

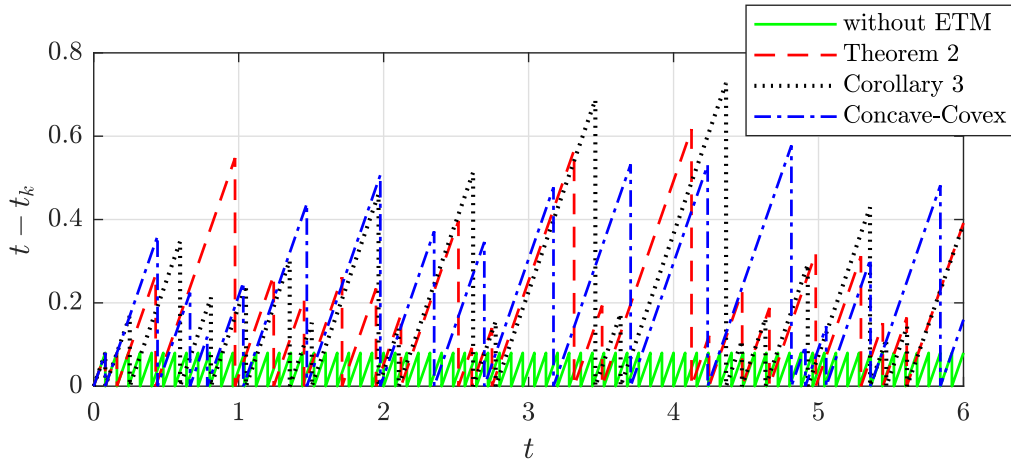


Figure 6: Inter-events time interval of the ETMs for the cases: without ETM (100%), Theorem 2 (31%), Corollary 3 (28%) and Concave-Convex technique (23%).

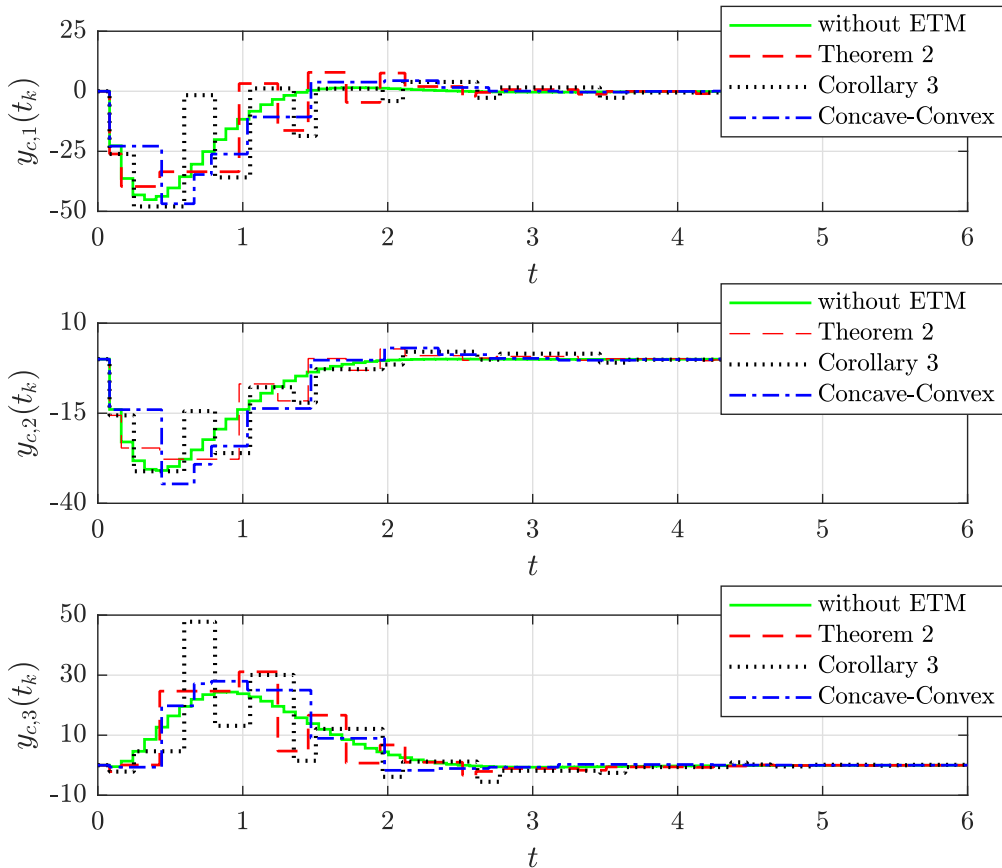


Figure 7: Control outputs.

with a tuning positive parameter T . Future work could be dedicated to expand the results to the co-design case of both the controller and anti-windup gain together with the parameters of the event-triggering mechanism, although it is clear that the co-design is definitively not a direct extension. Furthermore, we envision to study the behavior of the dynamic event-triggering mechanism when dealing with a control system with uncertainties.

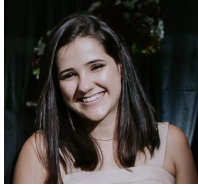
References

- [1] M. Abdelrahim, R. Postoyan, J. Daafouz, and D. Nešić. Stabilization of nonlinear systems using event-triggered output feedback controllers. *IEEE Transactions on Automatic Control*, 61(9):2682–2687, 2015.
- [2] K.J. Aström. Event based control. In *Analysis and design of nonlinear control systems*, pages 127–147. Springer-Verlag, Berlin Heidelberg, 2008.
- [3] C. Briat. Convergence and equivalence results for the Jensen’s inequality – application to time-delay and sampled-data systems. *IEEE Trans. Autom. Control*, 56(7):1660–1665, July 2011.
- [4] C. Briat and A. Seuret. A looped-functional approach for robust stability analysis of linear impulsive systems. *Systems & Control Letters*, 61(10):980–988, 2012.
- [5] C. De Souza, V.J.S. Leite, S. Tarbouriech, E. B. Castelan, and L.F.P. Silva. A direct parameter-error co-design approach of discrete-time saturated lpv systems. *IEEE Transactions on Automatic Control*, 2022.
- [6] Q. T. Dinh, S. Gumussoy, W. Michiels, and M. Diehl. Combining convex-concave decompositions and linearization approaches for solving bmis, with application to static output feedback. volume 57, pages 1377–1390. IEEE, 2011.
- [7] A. Girard. Dynamic triggering mechanisms for event-triggered control. *IEEE Trans. on Automatic Control*, 60(7):1992–1996, May 2015.
- [8] J. M. Gomes da Silva Jr, F.A. Bender, S. Tarbouriech, and J.M. Biannic. Dynamic anti-windup synthesis for state delayed systems: an lmi approach. In *Conference on Decision and Control (CDC)*, pages 6904–6909. IEEE, 2009.
- [9] W. P. M. H. Heemels, K.H. Johansson, and P. Tabuada. An introduction to event-triggered and self-triggered control. In *51th IEEE Conference on Decision and Control*, pages 3270 – 3285. Maui, Hawaii, December 2012.
- [10] J. Lunze and D. Lehmann. A state-feedback approach to event-based control. *Automatica*, 46(1):211–215, 2010.
- [11] L. G. Moreira, L. B. Groff, J. M. Gomes da Silva, and S. Tarbouriech. Event-triggered PI control for continuous plants with input saturation. In *American Control Conference (ACC)*, pages 4251–4256. IEEE, 2016.
- [12] L. G. Moreira, L. B. Groff, J. M. Gomes da Silva Jr, and S. Tarbouriech. Pi event-triggered control under saturating actuators. *International Journal of Control*, 92(7):1634–1644, 2019.
- [13] L.G. Moreira, S. Tarbouriech, A. Seuret, and J.M. Gomes da Silva Jr. Observer based event-triggered control in the presence of cone-bounded nonlinear inputs. *Nonlinear Analysis: Hybrid Systems*, 33:17–32, 2019.
- [14] R. Postoyan, P. Tabuada, D. Nešić, and A. Anta. A framework for the event-triggered stabilization of nonlinear systems. *IEEE Transactions on Automatic Control*, 60(4):982–996, 2014.
- [15] A. Seuret. A novel stability analysis of linear systems under asynchronous samplings. *Automatica*, 48(1):177 – 182, 2012.
- [16] A. Seuret and J.-M. Gomes da Silva Jr. Taking into account period variations and actuator saturation in sampled-data systems. *Systems & Control Letters*, 61(12):1286–1293, 2012.
- [17] A. Seuret, C. Prieur, S. Tarbouriech, and L. Zaccarian. LQ-based event-triggered controller co-design for saturated linear systems. *Automatica*, 74:47–54, 2016.
- [18] P. Tabuada. Event-triggered real-time scheduling of stabilizing control tasks. *IEEE Trans. on Automatic Control*, 52(9):1680–1685, 2007.
- [19] P. Tallapragada and N. Chopra. Event-triggered dynamic output feedback control of LTI systems. In *51th IEEE Conference on Decision and Control*, pages 6597–6602. Maui, Hawaii, December 2012.
- [20] P. Tallapragada and N. Chopra. On event triggered tracking for nonlinear systems. *IEEE Trans. on Automatic Control*, 58(9):2343–2348, September 2013.
- [21] S. Tarbouriech, G. Garcia, J.-M. Gomes da Silva Jr, and I. Queinnec. *Stability and Stabilization of Linear Systems with Saturating Actuators*. Springer, London, 2011.
- [22] S. Tarbouriech and A. Girard. Lmi-based design of dynamic event-triggering mechanism for linear systems. In *IEEE Conference on Decision and Control (CDC)*, pages 121–126. Miami, USA, December 2018.
- [23] S. Tarbouriech, A. Seuret, J.-M. Gomes da Silva Jr., and D. Sbarbaro. Observer-based event-triggered control co-design for linear systems. *IET Control Theory & Applications*, 10(18):2466–2473, 2016.
- [24] X. Wang and M. D. Lemmon. Event design in event-triggered feedback control systems. In *47th IEEE Conference on Decision and Control*, pages 2105–2110. IEEE, 2008.
- [25] Y. Yamamoto. New approach to sampled-data control systems - a function space method. In *Proceedings of the IEEE Conference on Decision and Control*, pages 1882–1887. Honolulu, December 1990. IEEE.
- [26] J. Zhang and G. Feng. Event-driven observer-based output feedback control for linear systems. *Automatica*, 50(7):1852–1859, 2014.

CRedit authorship contribution statement

Carla de Souza: Conceptualization, Methodology, Software, Validation, Formal analysis, Writing - original draft, review & editing. **Sophie Tarbouriech:** Conceptualization, Methodology, Formal analysis, Writing - original draft, review & editing, Supervision. **Isabelle Queinnec:** Conceptualization, Methodology, Formal analysis, Writing -

original draft, review & editing, Supervision. **Antoine Girard:** Conceptualization, Methodology, Formal analysis, Writing - original draft, review & editing, Supervision.



Carla de Souza was born in Barroso (MG, Brazil). She received her B.S. degree on Mechatronics Engineering from the CEFET-MG Divinópolis (MG, Brazil) in 2015, her M.S degree in Electrical Engineering from the CEFET–MG Belo-Horizonte (MG, Brazil) in 2017 and her Ph.D. degree in Automation and Systems Engineering from the Federal University of Santa Catarina (SC, Brazil) in 2021. She joined the MAC group at LAAS-CNRS (Toulouse, France) as a post-doctoral student in 2022. She is currently working in the R&D department of Leyfa Measurement, a subsidiary of SCNF, in Toulouse.



Sophie Tarbouriech received the Ph.D. degree in Control Theory in 1991 and the HDR degree (Habilitation à Diriger des Recherches) in 1998 from University Paul Sabatier, Toulouse, France. Currently, she is a Senior Researcher at CNRS and a member of LAAS-CNRS, Toulouse. Her main research interests include analysis and control of linear and nonlinear systems with constraints (limited information), hybrid dynamical systems. She is currently Associate Editor for SIAM Journal of Control and Optimization. She is also Senior Editor for IEEE Control Systems Letters and Automatica. She is also Deputy Editor-in-Chief of Automatica. She is also a member of IFAC and IEEE Technical Committees on Nonlinear Systems and Hybrid Systems.



Isabelle Queinnec is currently CNRS researcher at LAAS-CNRS, Toulouse University. She received her PhD degree and HDR degree in automatic control in 1990 and 2000, respectively, from University Paul Sabatier, Toulouse. Her current research interests include constrained control and robust control of processes with limited information, with particular interest in applications on aeronautical systems, robotic, electronic, biochemical and environmental processes. She has been serving as member of the IFAC technical committees on “Biosystems and Bioprocesses” and on “Modelling and Control of Environmental Systems”, respectively from 2002 and 2005 and of the IEEE CSS-CEB from 2013. She is currently AE for IEEE Transactions on Automatic Control. She is co-author of a book on saturated systems and of more than 50 journal papers, both in control theory and process engineering.



Antoine Girard is a Senior Researcher at CNRS and a member of the Laboratory of Signals and Systems. He received the Ph.D. degree in applied mathematics from Grenoble Institute of Technology, in 2004. From 2004 to 2006, he held postdoctoral positions at University of Pennsylvania and Université Grenoble-Alpes. From 2006 to 2015, he was an Assistant/Associate Professor at the Université Grenoble-Alpes. His main research interests deal with analysis and control of hybrid systems with an emphasis on computational approaches, formal methods and applications to cyber-physical systems. He received the George S. Axelby Outstanding Paper Award from the IEEE Control Systems Society in 2009. In 2014, he was awarded the CNRS Bronze Medal. In 2015, he was appointed as a junior member of the Institut Universitaire de France (IUF). In 2016, he was awarded an ERC Consolidator Grant. In 2018, he received the first HSCC Test of Time Award and the European Control Award.